

**PROCEEDINGS OF
THE ROYAL SOCIETY B**

BIOLOGICAL SCIENCES

The human visual system preserves the hierarchy of 2-dimensional pattern regularity

Journal:	<i>Proceedings B</i>
Manuscript ID	RSPB-2021-1142.R1
Article Type:	Research
Date Submitted by the Author:	29-Jun-2021
Complete List of Authors:	Kohler, Peter; York University - Keele Campus, Psychology Clarke, Alasdair; University of Essex
Subject:	Neuroscience < BIOLOGY, Cognition < BIOLOGY
Keywords:	symmetry, regular textures, steady-state EEG, psychophysics, visual processing
Proceedings B category:	Neuroscience & Cognition

SCHOLARONE™
Manuscripts

Author-supplied statements

Relevant information will appear here if provided.

Ethics

Does your article include research that required ethical approval or permits?:

Yes

Statement (if applicable):

Informed consent was obtained from all participants prior to data collection. For the EEG experiment the protocol was approved by the Institutional Review Board of Stanford University. For the psychophysics experiment the protocol was approved by the University of Essex's Ethics Committee.

Data

It is a condition of publication that data, code and materials supporting your paper are made publicly available. Does your paper present new data?:

Yes

Statement (if applicable):

In accordance with best practices of Open Science, the Supplementary Materials include all of the data and code required to run our analyses, as well as additional helpful figures and tables (see: <https://osf.io/f3ex8/>). For the convenience of the editor and reviewers, we are also uploading our Supplementary Materials as an html file with this submission as well as making it available to the public.

Conflict of interest

I/We declare we have no competing interests

Statement (if applicable):

CUST_STATE_CONFLICT :No data available.

Authors' contributions

CUST_AUTHOR CONTRIBUTIONS QUESTION :No data available.

Statement (if applicable):

CUST_AUTHOR CONTRIBUTIONS TEXT :No data available.

The human visual system preserves the hierarchy of 2-dimensional pattern regularity

Peter J. Kohler^{1,2,3} and Alasdair D. F. Clarke⁴

¹ York University, Department of Psychology, Toronto, ON M3J 1P3, Canada

² Centre for Vision Research, York University, Toronto, ON, M3J 1P3, Canada

³ Stanford University, Department of Psychology, Stanford, CA 94305, United States

⁴ University of Essex, Department of Psychology, Colchester, UK, CO4 3SQ

Abstract

Symmetries are present at many scales in natural scenes. Humans and other animals are highly sensitive to visual symmetry, and symmetry contributes to numerous domains of visual perception. The four fundamental symmetries, reflection, rotation, translation and glide reflection, can be combined into exactly 17 distinct regular textures. These *wallpaper groups* represent the complete set of symmetries in 2D images. The current study seeks to provide a more comprehensive description of responses to symmetry in the human visual system, by collecting both brain imaging (Steady-State Visual Evoked Potentials measured using high-density EEG) and behavioral (symmetry detection thresholds) data using the entire set of wallpaper groups. This allows us to probe the hierarchy of complexity among wallpaper groups, in which simpler groups are subgroups of more complex ones. We find that both behavior and brain activity preserve the hierarchy almost perfectly: Subgroups consistently produce lower amplitude symmetry-specific responses in visual cortex and require longer presentation durations to be reliably detected. These findings expand our understanding of symmetry perception by showing that the human brain encodes symmetries with a high level of precision and detail. This opens new avenues for research on how fine-grained representations of regular textures contribute to natural vision.

Symmetries are abundant in natural and man-made environments, due to a complex interplay of physical forces that govern pattern formation in nature. Sensitivity to symmetry has been demonstrated in a number of species, includes bees (Giurfa et al., 1996), fish (Morris and Casey, 1998; SchlÃijter et al., 1998), birds (MÃ¤ller, 1992; Swaddle and Cuthill, 1994) and dolphins (von Fersen et al., 1992), and may be used as a cue for mate selection in many species (Swaddle, 1999) including humans (Rhodes et al., 1998). Humans cultures have created and appreciated symmetrical patterns throughout history, and since the gestalt movement of the early 20th century, symmetry has been recognized as important for visual perception. Symmetry contributes to the perception of shapes (Palmer, 1985; Li et al., 2013), scenes (Apthorp and Bell, 2015) and surface properties (Cohen and Zaidi, 2013). This literature is almost exclusively based on stimuli in which one or more symmetry axes are placed at a single point in the image. Focus has been on mirror symmetry or *reflection*, with relatively few studies including the other fundamental symmetries: *rotation*, *translation* and *glide reflection* (Wagemans, 1998) - perhaps because reflection has been found to be more perceptually salient

37 (Mach, 1959; Royer, 1981; Palmer, 1991; Ogden et al., 2016; Hamada and Ishihara, 1988) and produce
38 more brain activity (Makin et al., 2013, 2014, 2012; Wright et al., 2015). In the current study, we
39 take a different approach by investigating visual processing of regular textures in which combinations
40 of the four fundamental symmetries tile the 2D plane.

41 In the two spatial dimensions relevant for images, symmetries can be combined in 17 distinct
42 ways, *the wallpaper groups* (Fedorov, 1891; Polya, 1924; Liu et al., 2010). Previous work on a sub-
43 set of four of the wallpaper groups used functional MRI to demonstrate that rotation symmetries in
44 wallpapers elicit parametric responses in several areas in occipital cortex, beginning with visual area
45 V3 (Kohler et al., 2016). This effect was also robust when symmetry responses were measured with
46 electroencephalography (EEG) using both Steady-State Visual Evoked Potentials (SSVEPs)(Kohler
47 et al., 2016) and Event-Related Potentials (Kohler et al., 2018). The SSVEP technique uses periodic
48 visual stimulation to produce a periodic brain response that is confined to integer multiples of the stim-
49 ulation frequency known as harmonics. SSVEP response harmonics can be isolated in the frequency
50 domain and depending on the specific design, different harmonics will express different aspects of the
51 brain response. (Norcia et al., 2015). Here we extend on the previous work by collecting SSVEPs and
52 psychophysical data from human participants viewing the full set of wallpaper groups. We measure
53 responses in visual cortex to 16 out of the 17 wallpaper groups, with the 17th serving as a control
54 stimulus. Our goal is to provide a more complete picture of how wallpaper groups are represented in
55 the human visual system.

56 A wallpaper group is a topologically discrete group of isometries of the Euclidean plane, i.e.
57 transformations that preserve distance (Liu et al., 2010). The wallpaper groups differ in the number
58 and kind of these transformations and we can uniquely refer to different groups using crystallographic
59 notation. In brief, most groups are notated by PXZ , where $X \in \{1, 2, 3, 4, 6\}$ indicates the highest
60 order of rotation symmetry and $Z \in \{m, g\}$ indicates whether the pattern contains reflection (m) or
61 glide reflection (g). For example, $P4$ contains rotation of order 4, while $P4MM$ contains rotation
62 of order 4 and two reflections. By convention, many of the groups are given shortened names: for
63 example, $P4MM$ is usually referred to as $P4M$, as the second reflection can be deduced from the
64 presence of rotation of order 4 alongside a reflection. Two of the groups start with a C rather than
65 a P , (CM and CMM) which indicates that the symmetries are specified relative to a cell that itself
66 contains repetition. Full details of the naming convention can be found on [wikipedia](#) and examples of
67 the wallpaper groups are shown in Figures 1 and 2.

68 In mathematical group theory, when the elements of one group is completely contained in another,
69 the inner group is called a subgroup of the outer group (Liu et al., 2010). The full list of subgroup
70 relationships is listed in Section 1.4.2 of the Supplementary Material. Subgroup relationships between
71 wallpaper groups can be distinguished by their indices. The index of a subgroup relationship is the
72 number of cosets, i.e. the number of times the subgroup is found in the supergroup (Liu et al., 2010).
73 As an example, let us consider groups $P2$ and $P6$ (see Figure 1B). If we ignore the translations in two
74 directions that both groups share, group $P6$ consists of the set of rotations $\{0^\circ, 60^\circ, 120^\circ, 180^\circ, 240^\circ,$
75 $300^\circ\}$, in which $P2$ $\{0^\circ, 180^\circ\}$ is contained. $P2$ is thus a subgroup of $P6$, and $P6$ can be generated
76 by combining $P2$ with rotations $\{0^\circ, 120^\circ, 240^\circ\}$. Because $P2$ is repeated three times in $P6$, $P2$ is a
77 subgroup of $P6$ with index 3 (Liu et al., 2010). Similarly, PMM contains two reflections and rotations

78 $\{0^\circ, 180^\circ\}$. PMM can be generated by adding an additional reflection to both $P2$ ($\{0^\circ, 180^\circ\}$) and
 79 PM (one reflection), so $P2$ and PM are both subgroups of PMM with index 2 (see Figure 1C). The
 80 17 wallpaper groups thus obey a hierarchy of complexity where simpler groups are subgroups of more
 81 complex ones (Coxeter and Moser, 1972).

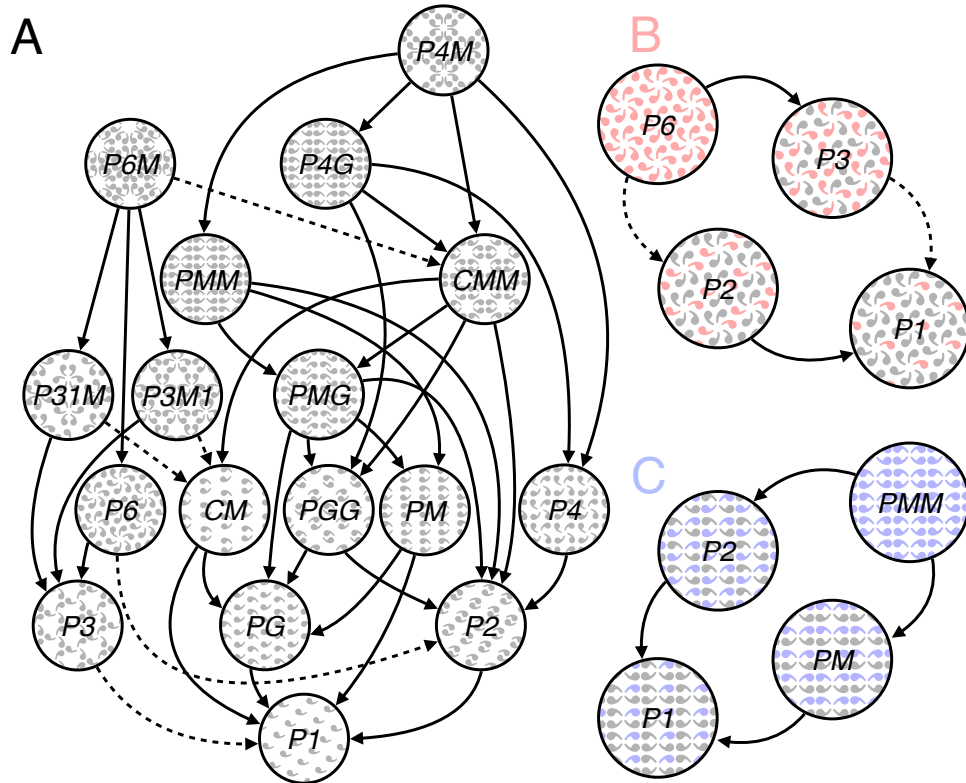


Figure 1: Subgroup relationships with indices 2 (solid lines) and 3 (dashed line) are shown in (A). All other relationships can be inferred by identifying the shortest path through the hierarchy, and multiplying the subgroup indices. For example, $P1$ is related to $P6$ through $P6 \rightarrow P3$ (index 2) and $P3 \rightarrow P1$ (index 3) so $P1$ is also a subgroup of $P6$ with index $3 \times 2 = 6$. We also show enlarged versions of some of the subgroup relationships involving $P6$ (B, shown in red) and PMM (C, shown in blue) and highlight the symmetries within the subgroups to emphasize how the supergroup can be generated by adding additional transformations to the subgroup. Illustration adapted from Wade (1993).

82 The two datasets we present here (data and analysis code has been made available on [OSF](#)) make
 83 it possible to assess the extent to which both behavior and brain responses follow the hierarchy of
 84 complexity expressed by the subgroup relationships. Based on previous brain imaging work showing
 85 that patterns with more axes of symmetry produce greater activity in visual cortex (Sasaki et al.,
 86 2005; Tyler et al., 2005; Kohler et al., 2018, 2016; Keefe et al., 2018), we hypothesized that more
 87 complex groups would produce larger SSVEPs. For the psychophysical data, we hypothesized that
 88 more complex groups would lead to shorter symmetry detection thresholds, based on previous data
 89 showing that under a fixed presentation time, discriminability increases with the number of symmetry
 90 axes in the pattern (Wagemans et al., 1991). Our results confirm both hypotheses, and show that
 91 activity in human visual cortex is remarkably consistent with the hierarchical relationships between the
 92 wallpaper groups, with SSVEP amplitudes and psychophysical thresholds following these relationships

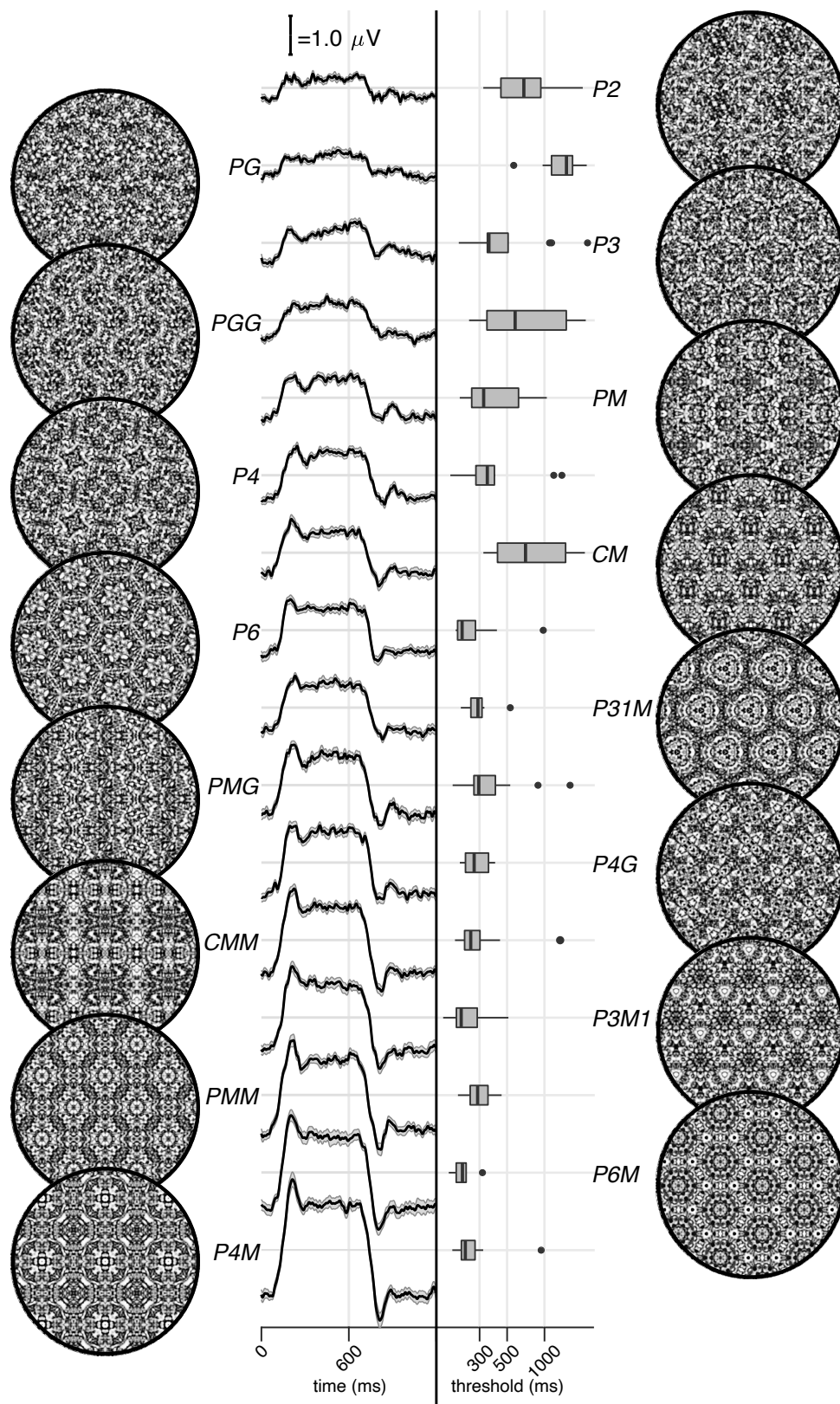


Figure 2: Examples of each of the 16 wallpaper groups are shown in the left- and right-most column of the figures, next to the corresponding SSVEP (center-left) and psychological (center-right) data from each group. The SSVEP data are odd-harmonic-filtered cycle-average waveforms. In each cycle, a *P1* exemplar was shown for the first 600 ms, followed by the original exemplar for the last 600 ms. Errorbars are standard error of the mean. Psychophysical data are presented as boxplots reflecting the distribution of display duration thresholds. The 16 groups are ordered by the strength of the SSVEP response, to highlight the range of response amplitudes.

93 at a level that is far beyond chance. The human visual system thus appears to encode all of the
94 fundamental symmetries using a representational structure that closely approximates the subgroup
95 relationships from group theory.

96 Results

97 The stimuli used in our two experiments were generated from random-noise textures, which made
98 it possible to generate multiple exemplars from each of the wallpaper groups, as described in detail
99 elsewhere (Kohler et al., 2016). We generated control stimuli matched to each exemplar in the main
100 stimulus set, by scrambling the phase but maintaining the power spectrum. All wallpaper groups
101 are inherently periodic because of their repeating lattice structure. Phase scrambling maintains this
102 periodicity, so the phase-scrambled control images all belong to group *P1* regardless of group mem-
103 bership of the original exemplar. *P1* contains no symmetries other than translation, while all other
104 groups contain translation in combination with one or more of the other three fundamental symmetries
105 (reflection, rotation, glide reflection) (Liu et al., 2010). In our SSVEP experiment, this stimulus set
106 allowed us to isolate brain activity specific to the symmetry structure in the exemplar images from
107 activity associated with modulation of low-level features, by alternating exemplar images and control
108 exemplars. In this design, responses to structural features beyond the shared power spectrum, includ-
109 ing any symmetries other than translation, are isolated in the odd harmonics of the image update
110 frequency (Kohler et al., 2016; Norcia et al., 2015, 2002). Thus, the combined magnitude of the odd
111 harmonic response components can be used as a measure of the overall strength of the visual cortex
112 response.

113 The psychophysical experiment took a distinct but related approach. In each trial an exemplar
114 image was shown with its matched control, one image after the other, and the order varied pseudo-
115 randomly such that in half the trials the original exemplar was shown first, and in the other half the
116 control image was shown first. After each trial, participants were instructed to indicate whether the
117 first or second image contained more structure. The duration of both images was controlled by a
118 staircase procedure so that a threshold duration for symmetry detection could be computed for each
119 wallpaper group.

120 Examples of the wallpaper groups and a summary of our brain imaging and psychophysical mea-
121 surements are shown in Figure 2. For our primary SSVEP analysis, we only considered EEG data
122 from a pre-determined region-of-interest (ROI) consisting of six electrodes over occipital cortex (see
123 Supplementary Figure 1.1). SSVEP data from this ROI was filtered so that only the odd harmonics
124 that capture the symmetry response contribute to the waveforms. While waveform amplitude is quite
125 variable among the 16 groups, all groups have a sustained negative-going response that begins at
126 about the same time for all groups, 180 ms after the transition from the *P1* control exemplar to
127 the original exemplar. To reduce the amplitude of the symmetry-specific response to a single number
128 that could be used in further analyses and compared to the psychophysical data, we computed the
129 root-mean-square (RMS) over the odd-harmonic-filtered waveforms. The data in Figure 2 are shown
130 in descending order according to RMS. The psychophysical results, shown in box plots in Figure 2,
131 were also quite variable between groups, and there seems to be a general pattern where wallpaper

132 groups near the top of the figure, that have lower SSVEP amplitudes, also have longer psychophysical
133 threshold durations.

134 We now wanted to test our two hypotheses about how SSVEP amplitudes and threshold durations
135 would follow subgroup relationships, and thereby quantify the degree to which our two measurements
136 were consistent with the group theoretical hierarchy of complexity. We tested each hypothesis using
137 the same approach. We first fitted a Bayesian model with wallpaper group as a factor and participant
138 as a random effect. We fit the model separately for SSVEP RMS and psychophysical data and then
139 computed posterior distributions for the difference between supergroup and subgroup. These difference
140 distributions allowed us to compute the conditional probability that the supergroup would produce
141 (a) larger RMS and (b) a shorter threshold durations, when compared to the subgroup. The posterior
142 distributions are shown in Figure 3 for the SSVEP data, and in Figure 4 for the psychophysical
143 data, which distributions color-coded according to conditional probability. For both data sets our
144 hypothesis is confirmed: For the overwhelming majority of the 63 subgroup relationships, supergroups
145 are more likely to produce larger symmetry-specific SSVEPs and shorter symmetry detection threshold
146 durations, and in most cases the conditional probability of this happening is extremely high.

147 We also ran a control analysis using (1) odd-harmonic SSVEP data from a six-electrode ROI over
148 parietal cortex (see Supplementary Figure 1.1) and (2) even-harmonic SSVEP data from the same
149 occipital ROI that was used in our primary analysis. By comparing these two control analysis to our
150 primary SSVEP analysis, we can address the specify of our effects in terms of location (occipital cortex
151 vs parietal cortex) and harmonic (odd vs even). For both control analyses (plotted in Supplementary
152 Figures 3.3 and 3.4), the correspondence between data and subgroup relationships was substantially
153 weaker than in the primary analysis. We can quantify the strength of the association between the
154 data and the subgroup relationships, by asking what proportion of subgroup relationships that reach
155 or exceed a range of probability thresholds. This is plotted in Figure 5, for our psychophysical data,
156 our primary SSVEP analysis and our two control SSVEP analyses. It shows that odd-harmonic
157 SSVEP data from the occipital ROI and symmetry detection threshold durations both have a strong
158 association with the subgroup relationships such that a clear majority of the subgroups survive even
159 at the highest threshold we consider ($p(\Delta > 0 | \text{data}) > 0.99$). The association is far weaker for the
160 two control analyses.

161 SSVEP data from four of the wallpaper groups ($P2$, $P3$, $P4$ and $P6$) was previously published
162 as part of our earlier demonstration of parametric responses to rotation symmetry in wallpaper
163 groups (Kohler et al., 2016). We replicate that result using our Bayesian approach, and find an analo-
164 gous parametric effect in the psychophysical data (see Supplementary Figure 4.1). We also conducted
165 an analysis testing for an effect of index in our two datasets and found that subgroup relationships with
166 higher indices tended to produce greater pairwise differences between the subgroup and supergroup,
167 for both SSVEP RMS and symmetry detection thresholds (see Supplementary Figure 4.2). The effect
168 of index is relatively weak, but the fact that there is a measurable index effect can nonetheless be taken
169 as preliminary evidence that representations of symmetries in wallpaper groups may be compositional.

170 Finally, we conducted a correlation analysis comparing SSVEP and psychophysical data and found
171 a reliable correlation ($R^2 = 0.44$, Bayesian confidence interval [0.28, 0.55]). The correlation reflects
172 an inverse relationship: For subgroup relationships where the supergroup produces a much *larger*

173 SSVEP amplitude than the subgroup, the supergroup also tends to produce a much *smaller* symmetry
174 detection threshold. This is consistent with our hypotheses about how the two measurements relate
175 to symmetry representations in the brain, and suggests that our brain imaging and psychophysical
176 measurements are at least to some extent tapping into the same underlying mechanisms.

177 Discussion

178 Here we show that beyond merely responding to the elementary symmetry operations of reflection
179 (Sasaki et al., 2005; Tyler et al., 2005) and rotation (Kohler et al., 2016), the visual system repre-
180 sents the hierarchical structure of the 17 wallpaper groups, and thus every combination of the four
181 fundamental symmetries (rotation, reflection, translation, glide reflection) which comprise the set of
182 regular textures. Both SSVEP amplitudes and symmetry detection thresholds preserve the hierarchy
183 of complexity among the wallpaper groups that is captured by the subgroup relationships (Coxeter
184 and Moser, 1972). For the SSVEP, this remarkable consistency was specific to the odd harmonics
185 of the stimulus frequency that are known to capture the symmetry-specific response (Kohler et al.,
186 2016) and to electrodes in a region-of-interest (ROI) over occipital cortex. When the same analysis
187 was done using the odd harmonics from electrodes over parietal cortex (Supplementary Figure 3.3)
188 or even harmonics from electrodes over occipital cortex (Supplementary Figure 3.4), the data was
189 substantially less consistent with the subgroup relationships (yellow and green lines, Figure 5).

190 The current study uses 16 distinct wallpaper groups, while previous neuroimaging studies focused
191 on a subset of 4 (Kohler et al., 2016, 2018). This represents a significant conceptual advance, because
192 it makes it possible to investigate the complete subgroup hierarchy among the 17 groups and ask to
193 what extent the hierarchy is reflected in brain activity. Our data provide a description of the visual
194 systemâŽs response to the complete set of symmetries in the two-dimensional plane. We do not
195 independently measure the response to *P1*, but because each of the 16 other groups produce non-zero
196 odd harmonic amplitudes (see Figure 2), we can conclude that the relationships between *P1* and all
197 other groups, where *P1* is the subgroup, are also preserved by the visual system. The subgroup
198 relationships are in many cases not obvious perceptually, and most participants had no knowledge
199 of group theory. Thus, the visual systemâŽs ability to preserve the subgroup hierarchy does not
200 depend on explicit knowledge of the relationships. Previous brain-imaging studies have found evidence
201 of parametric responses with the number of reflection symmetry folds Keefe et al. (2018); Sasaki et al.
202 (2005); Makin et al. (2016) and with the order of rotation symmetry Kohler et al. (2016). Our study
203 is the first demonstration that the brain encodes symmetry in this parametric fashion across every
204 possible combination of different *symmetry types*, and that this parametric encoding is also reflected in
205 behavior. Previous behavioral experiments have shown that although naïve observers can distinguish
206 many of the wallpaper groups (Landwehr, 2009), they tend to sort exemplars into fewer (4-12) sets
207 than the number of wallpaper groups, often placing exemplars from different wallpaper groups in
208 the same set (Clarke et al., 2011). The two-interval forced choice approach we use in the current
209 psychophysical experiment makes it possible to directly compare symmetry detection thresholds to
210 the subgroup hierarchy, and reveals that not only can the 17 wallpaper groups be distinguished based
211 on behavioral data, behavior largely follows the subgroup hierarchy.

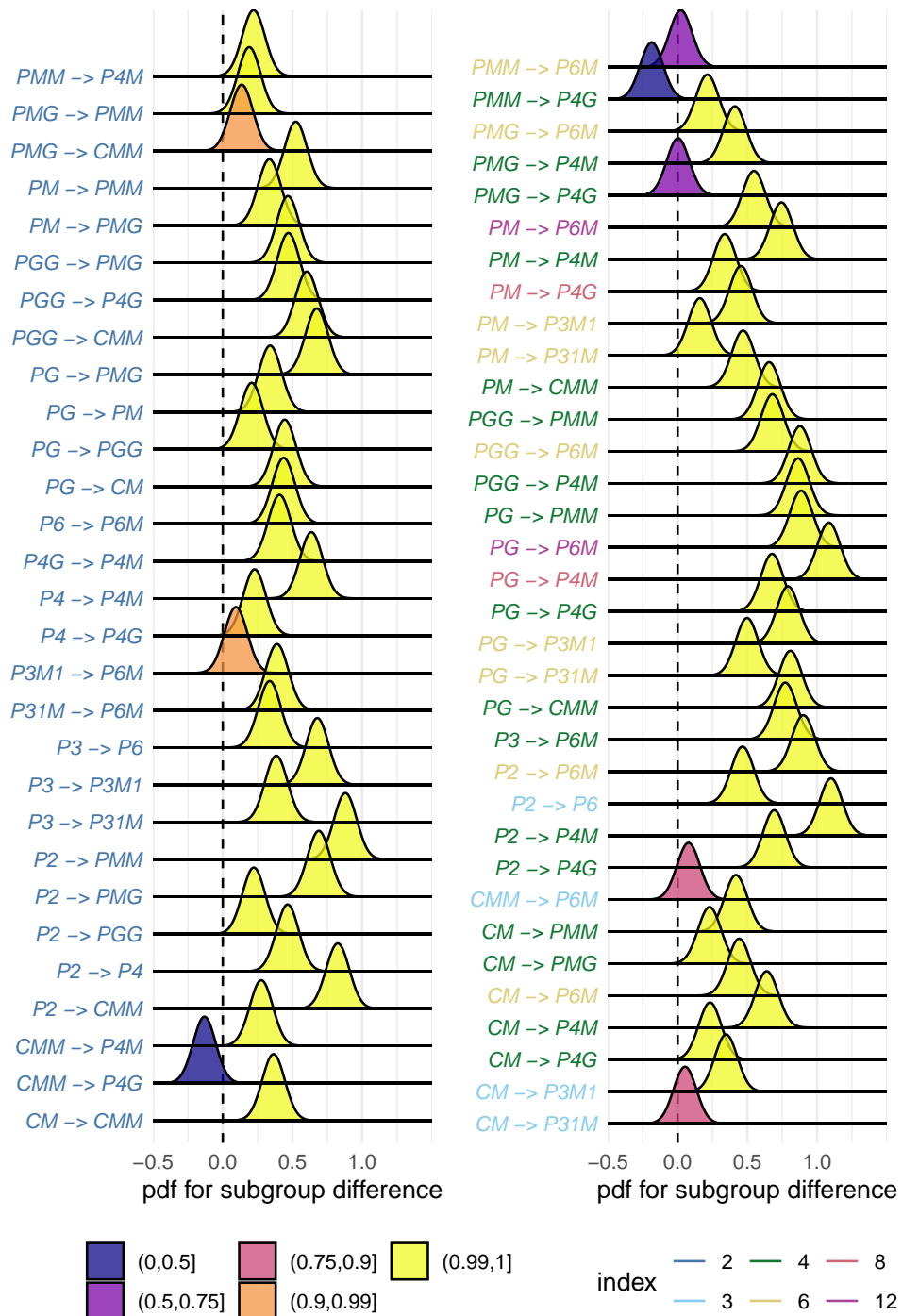


Figure 3: Posterior distributions for the difference in mean SSVEP RMS amplitude. Colour coding of the text indicates the index of the subgroup, while the colour of the filled distribution relates to the conditional probability that the difference in means is greater than zero. We can see that 55/63 subgroup relationships have $p(\Delta > 0 | \text{data}) > 0.99$.

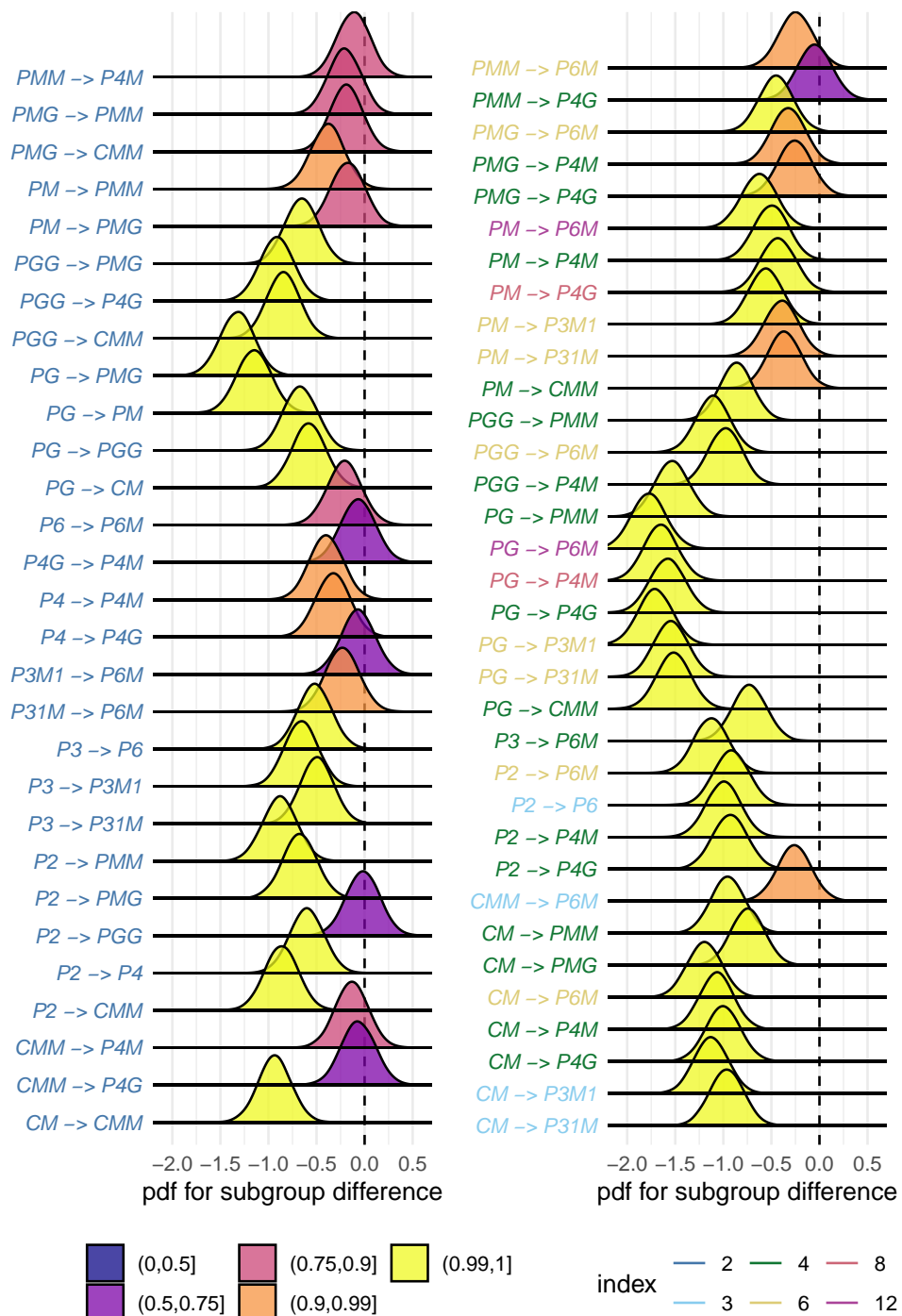


Figure 4: Posterior distributions for the difference in mean symmetry detection threshold durations. Colour coding of the text indicates the index of the subgroup, while the colour of the filled distribution relates to the conditional probability that the difference in means is smaller than zero. We can see that 43/63 subgroup relationships have $p(\Delta < 0 | \text{data}) > 0.99$.

212 A large literature exists on the *Sustained Posterior Negativity* (SPN), a characteristic negative-
213 going waveform that is known to reflect responses to symmetry and other forms of regularity and
214 structure (Makin et al., 2016). The SPN scales with the proportion of reflection symmetry in displays
215 that contain a mixture of symmetry and noise Makin et al. (2020); Palumbo et al. (2015), and both
216 reflection, rotation and translation can produce a measurable SPN Makin et al. (2013). It has recently
217 been demonstrated that a holographic model of regularity (van der Helm and Leeuwenberg, 1996), can
218 predict both SPN amplitude (Makin et al., 2016) and perceptual discrimination performance (Nucci
219 and Wagemans, 2007) for dot patterns that contain symmetry and other types of regularity. The
220 available evidence suggests that the SPN and our SSVEP measurements are two distinct methods
221 for isolating the same symmetry-related brain response: When observed in the time-domain, the
222 symmetry-selective odd-harmonic responses produce similarly sustained waveforms (see Figure 2),
223 odd-harmonic SSVEP responses can be measured for dot patterns similar to those used to measure
224 the SPN (Norcia et al., 2002), and the one event-related study on the wallpaper groups also found
225 SPN-like waveforms (Kohler et al., 2018). Future work should more firmly establish the connection
226 and determine if the SPN can capture similarly precise symmetry responses as the SSVEPs presented
227 here. It would also be worthwhile to ask if and how W can be computed for our random-noise based
228 wallpaper textures where combinations of symmetries tile the plane.

229 We observe a reliable correlation between our brain imaging and psychophysical data. This suggests
230 that the two measurements reflect the same underlying symmetry representations in visual cortex. It
231 should be noted that the correlation is relatively modest ($R^2 = 0.44$). This may be partly due to the fact
232 that different individuals participated in the two experiments. It may also be related to the fact
233 that participants were not doing a symmetry-related task during the SSVEP experiment, but instead
234 monitored the stimuli for brief changes in contrast that occurred twice per trial (see Methods). Previous
235 brain imaging studies have found enhanced reflection symmetry responses when participants performed
236 a symmetry-related task (Makin et al., 2020; Sasaki et al., 2005; Keefe et al., 2018). It is possible
237 that adding a symmetry-related task to our SSVEP experiment would have produced measurements
238 that reflected subgroup relationships to an even higher extent than what we observed. On the other
239 hand, our results are already close to ceiling (see Figure 5) and adding a symmetry-related task
240 may simply enhance SSVEP amplitudes overall without improving the discriminability of individual
241 groups, as has been observed for reflection by Keefe et al. (2018). Task-driven processing may be
242 important for detecting symmetries that have been subject to perspective distortion, as suggested by
243 SPN measurements (Makin et al., 2015) and somewhat less clearly in a subsequent functional MRI
244 study (Keefe et al., 2018). Future work in which behavioral and brain imaging data are collected from
245 the same participants, and task is manipulated in the SSVEP experiment, will help further establish
246 the connection between the two measurements, and elucidate the potential contribution of task-related
247 top-down processing to the current results.

248 We also find an effect of index for both our brain imaging measurements and our symmetry detec-
249 tion thresholds. This means that the visual system not only represents the hierarchical relationship
250 captured by individual subgroups, but also distinguishes between subgroups depending on how many
251 times the subgroup is repeated in the supergroup, with more repetitions leading to larger pairwise
252 differences. Our measured effect of index is relatively weak. This is perhaps because the index analy-

253 sis does not take into account the *type* of isometries that differentiate the subgroup and supergroup.
254 The effect of symmetry type can be observed by contrasting the measured SSVEP amplitudes and
255 detection thresholds for groups *PM* and *PG* in Figure 2. The two groups are comparable except *PM*
256 contains reflection and *PG* contains glide reflection, and the former clearly elicits higher amplitudes
257 and lower thresholds. An important goal for future work will be to map out how different symmetry
258 types contribute to the representational hierarchy.

259 The correspondence between responses in the visual system and group theory that we demonstrate
260 here, may reflect a form of implicit learning that depends on the structure of the natural world. The
261 environment is itself constrained by physical forces underlying pattern formation and these forces
262 are subject to multiple symmetry constraints (Hoyle, 2006). The ordered structure of responses to
263 wallpaper groups could be driven by a central tenet of neural coding, that of efficiency. If coding is to
264 be efficient, neural resources should be distributed to capture the structure of the environment with
265 minimum redundancy considering the visual geometric optics, the capabilities of the subsequent neural
266 coding stages and the behavioral goals of the organism (Attneave, 1954; Barlow, 1961; Laughlin, 1981;
267 Geisler et al., 2009). Early work within the efficient coding framework suggested that natural images
268 had a $1/f$ spectrum and that the corresponding redundancy between pixels in natural images could
269 be coded efficiently with a sparse set of oriented filter responses, such as those present in the early
270 visual pathway (Field, 1987; Olshausen and Field, 1997). Our results suggest that the principle of
271 efficient coding extends to a much higher level of structural redundancy – that of symmetries in
272 visual images.

273 The 17 wallpaper groups are completely regular, and relatively rare in the visual environment,
274 especially when considering distortions due to perspective (see above) and occlusion. Near-regular
275 textures, however, abound in the visual world, and can be modeled as deformed versions of the
276 wallpaper groups (Liu et al., 2004). The correspondence between visual cortex responses and group
277 theory demonstrated here may indicate that the visual system represents visual textures using a similar
278 scheme, with the wallpaper groups serving as anchor points in representational space. This framework
279 resembles norm-based encoding strategies that have been proposed for other stimulus classes, most
280 notably faces (Leopold et al., 2006), and leads to the prediction that adaptation to wallpaper patterns
281 should distort perception of near-regular textures, similar to the aftereffects found for faces (Webster
282 and MacLin, 1999). Field biologists have demonstrated that animals respond more strongly to exag-
283 gerated versions of a learned stimulus, referred to as “supernormal” stimuli (Tinbergen, 1953).
284 In the norm-based encoding framework, wallpaper groups can be considered *supertextures*, exaggerated
285 examples of the near-regular textures common in the natural world. If non-human animals employ a
286 similar encoding strategy, they would be expected to be sensitive to symmetries in wallpaper groups.
287 Recent functional MRI work in macaque monkeys offer some support for that: Macaque visual cortex
288 responds parametrically to reflection and rotation symmetries in wallpaper groups, and the set of brain
289 areas involved largely overlap those observed to be sensitive to symmetry in humans (Audurier et al.,
290 2021). In human societies, visual artists may consciously or unconsciously create supernormal stimuli,
291 to capture the essence of the subject and evoke strong responses in the audience (Ramachandran and
292 Hirstein, 1999). Wallpaper groups are visually compelling, and symmetries have been widely used in
293 human artistic expression going back to the Neolithic age (Jablan, 2014). If wallpapers are in fact

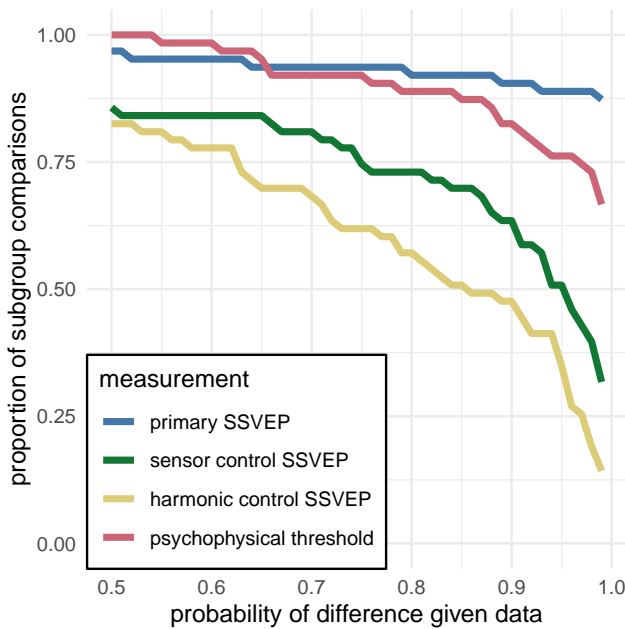


Figure 5: This plot shows the proportion of subgroup relationships that satisfy $p(\Delta > 0|data) > x$ for the SSVEP data and $p(\Delta < 0|data) > x$ for the psychophysical data. We can see that if we take $x = 0.95$ as our threshold, the subgroup relationships are preserved in $56/63 = 89\%$ and $48/63 = 76\%$ of the comparisons for the primary SSVEP and threshold duration datasets, respectively. This compares to the $32/63 = 51\%$ and $22/63 = 35\%$ for the SSVEP control datasets.

294 supertextures, this prevalence may be a direct result of the strategy the human visual system has
295 adopted for texture encoding.

296 Participants

297 Twenty-five participants (11 females, mean age 28.7 ± 3.3) took part in the EEG experiment. Their
298 informed consent was obtained before the experiment under a protocol that was approved by the
299 Institutional Review Board of Stanford University. 11 participants (8 females, mean age 20.73 ± 1.21)
300 took part in the psychophysics experiment. All participants had normal or corrected-to-normal vision.
301 Their informed consent was obtained before the experiment under a protocol that was approved by
302 the University of Essex's Ethics Committee. There was no overlap in participants between the EEG
303 and psychophysics experiments.

304 Stimulus Generation

305 Exemplars from the different wallpaper groups were generated using a modified version of the method-
306 ology developed by Clarke and colleagues (Clarke et al., 2011) that we have described in detail else-
307 where (Kohler et al., 2016). Briefly, exemplar patterns for each group were generated from random-
308 noise textures, which were then repeated and transformed to cover the plane, according to the sym-
309 metry axes and geometric lattice specific to each group. The use of noise textures as the starting point
310 for stimulus generation allowed the creation of an almost infinite number of distinct exemplars of each
311 wallpaper group. To make individual exemplars as similar as possible we replaced the power spectrum

of each exemplar with the median across exemplars within a group. We then generated control exemplars that had the same power spectrum as the exemplar images by randomizing the phase of each exemplar image. The phase scrambling eliminates rotation, reflection and glide-reflection symmetries within each exemplar, but the phase-scrambled images inherit the spectral periodicity arising from the periodic tiling. This means that all control exemplars, regardless of which wallpaper group they are derived from, are transformed into another symmetry group, namely $P1$. $P1$ is the simplest of the wallpaper groups and contains only translations of a region whose shape derives from the lattice. Because the different wallpaper groups have different lattices, $P1$ controls matched to different groups have different power spectra. Our experimental design takes these differences into account by comparing the neural responses evoked by each wallpaper group to responses evoked by the matched control exemplars.

Stimulus Presentation

Stimulus Presentation. For the EEG experiment, the stimuli were shown on a 24.5" Sony Trimaster EL PVM-2541 organic light emitting diode (OLED) display at a screen resolution of 1920×1080 pixels, 8-bit color depth and a refresh rate of 60 Hz, viewed at a distance of 70 cm. The mean luminance was 69.93 cd/m² and contrast was 95%. The diameter of the circular aperture in which the wallpaper pattern appeared was 13.8° of visual angle presented against a mean luminance gray background. Stimulus presentation was controlled using in-house software. For the psychophysics experiment, the stimuli were shown on a 48 × 27cm VIEWPixx/3D LCD Display monitor, model VPX-VPX-2005C, resolution 1920×1080 pixels, with a viewing distance of approximately 40cm and linear gamma. Stimulus presentation was controlled using MatLab and Psychtoolbox-3 (Kleiner et al., 2007; Brainard, 1997). The diameter of the circular aperture for the stimuli was 21.5°.

EEG Procedure

Visual Evoked Potentials were measured using a steady-state design, in which $P1$ control images alternated with exemplar images from each of the 16 other wallpaper groups. Exemplar images were always preceded by their matched $P1$ control image. A single 0.83 Hz stimulus cycle consisted of a control $P1$ image followed by an exemplar image, each shown for 600 ms. A trial consisted of 10 such cycles (12 sec) over which 10 different exemplar images and matched controls from the same rotation group were presented. For each group type, the individual exemplar images were always shown in the same order within the trials. Participants initiated each trial with a button-press, which allowed them to take breaks between trials. Trials from a single wallpaper group were presented in blocks of four repetitions, which were themselves repeated twice per session, and shown in random order within each session. To control fixation, the participants were instructed to fixate a small white cross in the center of display. To control vigilance, a contrast dimming task was employed. Two times per trial, an image pair (control $P1$ plus exemplar) was shown at reduced contrast. Participants were instructed to press a button on a response pad whenever they noticed a contrast change. Reaction times were not taken into account and participants were told to respond at their own pace while being as accurate as possible. We adjusted the reduction in contrast such that average accuracy for each participant was kept at 85% correct, in order to keep the difficulty of the vigilance task at a constant level.

351 Psychophysics Procedure

352 The experiment consisted of 16 blocks, one for each of the wallpaper groups (excluding *P1*). We used
353 a two-interval forced choice approach. In each trial, participants were presented with two stimuli (one
354 of which was the wallpaper group for the current block of trials, the other being *P1*), one after the
355 other (inter-stimulus interval of 700ms). After each stimulus had been presented, it was masked with
356 white noise for 300ms. After both stimuli had been presented, participants made a response on the
357 keyboard to indicate whether they thought the first or second image contained more symmetry. Each
358 block started with 10 practice trials, (stimulus display duration of 500ms) to allow participants to
359 familiarise themselves with the current block's wallpaper pattern. If they achieved an accuracy of
360 9/10 in these trials they progressed to the rest of the block, otherwise they carried out another set of
361 10 practise trials. This process was repeated until the required accuracy of 9/10 was obtained. The
362 rest of the block consisted of four interleaved staircases (using the QUEST algorithm ([Watson and](#)
[Pelli, 1983](#)), full details given in the SI) of 30 trials each. On average, a block of trials took around 10
364 minutes to complete.

365 EEG Acquisition and Preprocessing

366 Steady-State Visual Evoked Potentials (SSVEPs) were collected with 128-sensor HydroCell Sensor
367 Nets (Electrical Geodesics, Eugene, OR) and were band-pass filtered from 0.3 to 50 Hz. Raw data
368 were evaluated off line according to a sample-by-sample thresholding procedure to remove noisy sensors
369 that were replaced by the average of the six nearest spatial neighbors. On average, less than 5% of
370 the electrodes were substituted; these electrodes were mainly located near the forehead or the ears.
371 The substitutions can be expected to have a negligible impact on our results, as the majority of our
372 signal can be expected to come from electrodes over occipital, temporal and parietal cortices. After
373 this operation, the waveforms were re-referenced to the common average of all the sensors. The data
374 from each 12s trial were segmented into five 2.4 s long epochs (i.e., each of these epochs was exactly 2
375 cycles of image modulation). Epochs for which a large percentage of data samples exceeding a noise
376 threshold (depending on the participant and ranging between 25 and 50 μ V) were excluded from the
377 analysis on a sensor-by-sensor basis. This was typically the case for epochs containing artifacts, such as
378 blinks or eye movements. Steady-state stimulation will drive cortical responses at specific frequencies
379 directly tied to the stimulus frequency. It is thus appropriate to quantify these responses in terms of
380 both phase and amplitude. Therefore, a Fourier analysis was applied on every remaining epoch using
381 a discrete Fourier transform with a rectangular window. The use of two-cycle long epochs (i.e., 2.4 s)
382 was motivated by the need to have a relatively high resolution in the frequency domain, $\delta f = 0.42$ Hz.
383 For each frequency bin, the complex-valued Fourier coefficients were then averaged across all epochs
384 within each trial. Each participant did two sessions of 8 trials per condition, which resulted in a total
385 of 16 trials per condition.

386 SSVEP Analysis

387 Response waveforms were generated for each group by selective filtering in the frequency domain.
388 For each participant, the average Fourier coefficients from the two sessions were averaged over trials

and sessions. The SSVEP paradigm we used allowed us to separate symmetry-related responses from non-specific contrast transient responses. Previous work has demonstrated that symmetry-related responses are predominantly found in the odd harmonics of the stimulus frequency, whereas the even harmonics consist mainly of responses unrelated to symmetry, that arise from the contrast change associated with the appearance of the second image (Norcia et al., 2002; Kohler et al., 2016). This functional distinction of the harmonics allowed us to generate a single-cycle waveform containing the response specific to symmetry, by filtering out the even harmonics in the spectral domain, and then back-transforming the remaining signal, consisting only of odd harmonics, into the time-domain. For our main analysis, we averaged the odd harmonic single-cycle waveforms within a six-electrode region of interest (ROI) over occipital cortex (electrodes 70, 74, 75, 81, 82, 83). These waveforms, averaged over participants, are shown in Figure 2. The same analysis was done for the even harmonics and for the odd harmonics within a six electrode ROI over parietal cortex (electrodes 53, 54, 61, 78, 79, 86; see Supplementary Figure 1.1). The root-mean square values of these waveforms, for each individual participant, were used to determine whether each of the wallpaper subgroup relationships were preserved in the brain data.

Defining the list of subgroup relationships

In order to get the complete list of subgroup relationships, we digitized Table 4 from Coxeter (Coxeter and Moser, 1972) (shown in Supplementary Table 1.2). After removing identity relationships (i.e. each group is a subgroup of itself) and the three pairs of wallpaper groups that are subgroups of each other (e.g. *PM* is a subgroup of *CM*, and *CM* is a subgroup of *PM*) we were left with a total of 63 unambiguous subgroups that were included in our analysis.

Bayesian Analysis of SSVEP and Psychophysical data

Bayesian analysis was carried out using R (v3.6.1) (R Core Team, 2019) with the `brms` package (v2.9.0) (Bürkner, 2017) and rStan (v2.19.2 (Stan Development Team, 2019)). The data from each experiment were modelled using a Bayesian generalised mixed effect model with wallpaper group being treated as a 16-level factor, and random effects for participant. The SSVEP data and symmetry detection threshold durations were modelled using log-normal distributions with weakly informative, $\mathcal{N}(0, 2)$, priors. After fitting the model to the data, samples were drawn from the posterior distribution of the two datasets, for each wallpaper group. These samples were then recombined to calculate the distribution of differences for each of the 63 pairs of subgroup and supergroup. These distributions were then summarised by computing the conditional probability of obtaining a positive (or for the psychophysical data, negative) difference, $p(\Delta|\text{data})$. For further technical details, please see the Supplementary Materials where the full R code, model specification, prior and posterior predictive checks, and model diagnostics, can be found.

Acknowledgments

The authors would like to thank two anonymous reviewers whose comments helped improve and clarify the manuscript, and also express their gratitude to Professor Anthony M. Norcia for his invaluable

426 mentorship and contribution to our thinking about the role of symmetry in vision, and about vision and
 427 the brain more generally, through years of collaboration and discussions. This work was supported by
 428 the Vision Science to Applications (VISTA) program funded by the Canada First Research Excellence
 429 Fund (CFREF, 2016–2023) and by a Discovery Grant from the Natural Sciences and Engineering
 430 Research Council of Canada awarded to PJK. The work was also partially supported by a National
 431 Science Foundation INSPIRE grant 1248076 awarded to Yanxi Liu, Anthony M. Norcia and Rick O.
 432 Gilmore. A preliminary version of the EEG portion of the manuscript was previously deposited on
 433 [bioRxiv](#).

434 Data Accessibility

435 Data from the EEG and Psychophysics experiments have been made available with the Supplementary
 436 Material on [OSF](#).

437 References

- 438 Apthorp, D. and Bell, J. (2015). Symmetry is less than
 439 meets the eye. *Current Biology*, 25(7):R267–R268.
- 440 Attneave, F. (1954). Some informational aspects of
 441 visual perception. *Psychol Rev*, 61(3):183–93.
- 442 Audurier, P., HÅlja-Brichard, Y., Castro, V. D.,
 443 Kohler, P. J., Norcia, A. M., Durand, J.-B.,
 444 and Cottereau, B. R. (2021). Symmetry process-
 445 ing in the macaque visual cortex. *bioRxiv*, page
 446 2021.03.13.435181. Publisher: Cold Spring Harbo-
 447 r Laboratory Section: New Results.
- 448 Barlow, H. B. (1961). *Possible principles underlying
 449 the transformations of sensory messages*, pages 217–
 450 234. MIT Press.
- 451 Brainard, D. H. (1997). Spatial vision. *The ps-
 452 chophysics toolbox*, 10:433–436.
- 453 Bürkner, P.-C. (2017). Advanced bayesian multilevel
 454 modeling with the r package brms. *arXiv preprint arXiv:1705.11123*.
- 455 Clarke, A. D. F., Green, P. R., Halley, F., and
 456 Chantler, M. J. (2011). Similar symmetries: The
 457 role of wallpaper groups in perceptual texture simi-
 458 larity. *Symmetry*, 3(4):246–264.
- 459 Cohen, E. H. and Zaidi, Q. (2013). Symmetry in con-
 460 text: Salience of mirror symmetry in natural pat-
 461 terns. *Journal of vision*, 13(6).
- 462 Coxeter, H. S. M. and Moser, W. O. J. (1972). *Gen-
 463 erators and relations for discrete groups*. Ergebnisse
 464 der Mathematik und ihrer Grenzgebiete ; Bd. 14.
 465 Springer-Verlag, Berlin, New York.
- 466 Fedorov, E. (1891). Symmetry in the plane. In *Zapiski
 467 Imperatorskogo S. Peterburgskogo Mineralogichesko
 468 Obshchestva [Proc. S. Peterb. Mineral. Soc.]*, vol-
 469 ume 2, pages 345–390.
- 470 Field, D. J. (1987). Relations between the statistics of
 471 natural images and the response properties of corti-
 472 cal cells. *J Opt Soc Am A*, 4(12):2379–94.
- 473 Geisler, W. S., Najemnik, J., and Ing, A. D. (2009).
 474 Optimal stimulus encoders for natural tasks. *Jour-
 475 nal of Vision*, 9(13):17–17.
- 476 Giurfa, M., Eichmann, B., and Menzel, R. (1996).
 477 Symmetry perception in an insect. *Nature*,
 478 382(6590):458–461. Number: 6590 Publisher: Na-
 479 ture Publishing Group.
- 479 Hamada, J. and Ishihara, T. (1988). Complexity and
 480 goodness of dot patterns varying in symmetry. *Psy-
 481 chological Research*, 50(3):155–161.
- 482 Hoyle, R. B. (2006). *Pattern formation: an introduc-
 483 tion to methods*. Cambridge University Press.
- 484 Jablan, S. V. (2014). *Symmetry, Ornament and Modu-
 485 larity*. World Scientific Publishing Co Pte Ltd, Sin-
 486 gapore, SINGAPORE.
- 487 Keefe, B. D., Gouws, A. D., Sheldon, A. A., Vernon, R.
 488 J. W., Lawrence, S. J. D., McKeeffry, D. J., Wade,

- 491 A. R., and Morland, A. B. (2018). Emergence of
492 symmetry selectivity in the visual areas of the human
493 brain: fMRI responses to symmetry presented
494 in both frontoparallel and slanted planes. *Human
495 Brain Mapping*, 39(10):3813–3826. 535
- 496 Kleiner, M., Brainard, D., Pelli, D., Ingling, A., Murray,
497 R., and Broussard, C. (2007). What's new in
498 psychtoolbox-3. *Perception*, 36:1–16. 539
- 499 Kohler, P. J., Clarke, A., Yakovleva, A., Liu, Y., and
500 Norcia, A. M. (2016). Representation of maximally
501 regular textures in human visual cortex. *The Journal
502 of Neuroscience*, 36(3):714–729. 543
- 503 Kohler, P. J., Cottetereau, B. R., and Norcia, A. M.
504 (2018). Dynamics of perceptual decisions about sym-
505 metry in visual cortex. *NeuroImage*, 167(Supple-
506 ment C):316–330. 547
- 507 Landwehr, K. (2009). Camouflaged symmetry. *Percep-
508 tion*, 38:1712–1720. 549
- 509 Laughlin, S. (1981). A simple coding procedure en-
510 hances a neuron's information capacity. *Z Naturforsch C*, 36(9–10):910–2. 552
- 511 Leopold, D. A., Bondar, I. V., and Giese, M. A.
512 (2006). Norm-based face encoding by single neu-
513 rons in the monkey inferotemporal cortex. *Nature*,
514 442(7102):572–5. 556
- 515 Li, Y., Sawada, T., Shi, Y., Steinman, R., and Pizlo,
516 Z. (2013). *Symmetry Is the sine qua non of Shape*,
517 book section 2, pages 21–40. Advances in Computer
518 Vision and Pattern Recognition. Springer London, 560
- 519 Liu, Y., Hel-Or, H., Kaplan, C. S., and Van Gool, L.
520 (2010). Computational symmetry in computer vision
521 and computer graphics. *Foundations and Trends in
522 Computer Graphics and Vision*, 5(1–2):1–193. 564
- 523 Liu, Y., Lin, W.-C., and Hays, J. (2004). Near-regular
524 texture analysis and manipulation. In *ACM Trans-
525 actions on Graphics (TOG)*, volume 23, pages 368–
526 376. ACM. 568
- 527 Mach, E. (1959). *The Analysis of Sensations* (1897).
528 English transl., Dover, New York. 569
- 529 Makin, A. D. J., Rampone, G., and Bertamini, M.
530 (2015). Conditions for view invariance 570
- 531 in the neural response to visual symmetry. *Psychophysiology*, 52(4):532–543. eprint:
<https://onlinelibrary.wiley.com/doi/pdf/10.1111/psyp.12365>.
- Makin, A. D. J., Rampone, G., Morris, A., and
Bertamini, M. (2020). The Formation of Symmetri-
cal Gestalts Is Task-Independent, but Can Be En-
hanced by Active Regularity Discrimination. *Journal
of Cognitive Neuroscience*, 32(2):353–366.
- Makin, A. D. J., Rampone, G., Pecchinenda,
A., and Bertamini, M. (2013). Electrophysio-
logical responses to visuospatial regularity. *Psychophysiology*, 50(10):1045–1055. eprint:
<https://onlinelibrary.wiley.com/doi/pdf/10.1111/psyp.12082>.
- Makin, A. D. J., Rampone, G., Wright, A., Martinovic,
J., and Bertamini, M. (2014). Visual symmetry in
objects and gaps. *Journal of Vision*, 14(3):12–12.
- Publisher: The Association for Research in Vision
and Ophthalmology.
- Makin, A. D. J., Wilton, M. M., Pecchinenda, A., and
Bertamini, M. (2012). Symmetry perception and
affective responses: A combined EEG/EMG study.
Neuropsychologia, 50(14):3250–3261.
- Makin, A. D. J., Wright, D., Rampone, G., Palumbo,
L., Guest, M., Sheehan, R., Cleaver, H., and
Bertamini, M. (2016). An Electrophysiological
Index of Perceptual Goodness. *Cerebral Cortex*,
26(12):4416–4434.
- Morris, M. R. and Casey, K. (1998). Female sword-
tail fish prefer symmetrical sexual signal. *Animal
Behaviour*, 55(1):33–39.
- MÄÿller, A. P. (1992). Female swallow preference
for symmetrical male sexual ornaments. *Nature*,
357(6375):238–240.
- Norcia, A. M., Appelbaum, L. G., Ales, J. M., Cottetereau,
B. R., and Rossion, B. (2015). The steady-
state visual evoked potential in vision research: A
review. *Journal of Vision*, 15(6):4–4.
- Norcia, A. M., Candy, T. R., Pettet, M. W., Vildavski,
V. Y., and Tyler, C. W. (2002). Temporal dynam-
ics of the human response to symmetry. *Journal of
Vision*, 2(2):132–139.

- 573 Nucci, M. and Wagemans, J. (2007). Goodness of
 574 Regularity in Dot Patterns: Global Symmetry, Local
 575 Symmetry, and Their Interactions. *Perception*,
 576 36(9):1305–1319. Publisher: SAGE Publications Ltd
 577 STM. 619
- 578 Ogden, R., Makin, A. D. J., Palumbo, L., and
 579 Bertamini, M. (2016). Symmetry Lasts Longer
 580 Than Random, but Only for Brief Presentations.
 581 *i-Perception*, 7(6):2041669516676824. Publisher:
 582 SAGE Publications. 623
- 583 Olshausen, B. A. and Field, D. J. (1997). Sparse coding
 584 with an overcomplete basis set: a strategy employed
 585 by v1? *Vision Res*, 37(23):3311–25. 624
- 586 Palmer, S. E. (1985). The role of symmetry in shape
 587 perception. *Acta Psychologica*, 59(1):67–90. 628
- 588 Palmer, S. E. (1991). Goodness, Gestalt, groups, and
 589 Garner: Local symmetry subgroups as a theory of
 590 figural goodness. In *The perception of structures: Essays in honor of Wendell R. Garner*, pages 232
 591 39. American Psychological Association, Washington, DC, US. 629
- 594 Palumbo, L., Bertamini, M., and Makin, A. (2015).
 595 Scaling of the extrastriate neural response to sym-
 596 metry. *Vision Research*, 117:1–8. 634
- 597 Polya, G. (1924). Xii. AIJber die analogie der
 598 kristallsymmetrie in der ebene. *Zeitschrift fÃ¼r Kristallographie-Crystalline Materials*, 60(1):278–
 599 282. 637
- 601 R Core Team (2019). *R: A Language and Environment for Statistical Computing*. R Foundation for
 602 Statistical Computing, Vienna, Austria. 643
- 604 Ramachandran, V. S. and Hirstein, W. (1999). The
 605 science of art: A neurological theory of aesthetic
 606 experience. *Journal of Consciousness Studies*, 6(6–7):15–41. 644
- 608 Rhodes, G., Proffitt, F., Grady, J. M., and Sumich, A. (1998). Facial symmetry and the perception of
 609 beauty. *Psychonomic Bulletin & Review*, 5(4):659–669. 648
- 612 Royer, F. L. (1981). Detection of symmetry. *Journal of Experimental Psychology: Human Perception and Performance*, 7(6):1186–1210. 654
- 520 Sasaki, Y., Vanduffel, W., Knutsen, T., Tyler, C., and
 521 Tootell, R. (2005). Symmetry activates extrastriate visual cortex in human and nonhuman primates. *Proceedings of the National Academy of Sciences of the United States of America*, 102(8):3159–3163.
- 520 SchlÃijter, A., Parzefall, J., and Schlupp, I. (1998). Female preference for symmetrical vertical bars in male sailfin mollies. *Animal Behaviour*, 56(1):147–153.
- 520 Stan Development Team (2019). RStan: the R interface to Stan. R package version 2.19.2.
- 520 Swaddle, J. P. (1999). Visual signalling by asymmetry: a review of perceptual processes. *Philosophical Transactions of the Royal Society of London. Series B: Biological Sciences*. Publisher: The Royal Society.
- 520 Swaddle, J. P. and Cuthill, I. C. (1994). Preference for symmetric males by female zebra finches. *Nature*, 367(6459):165–166. Number: 6459 Publisher: Nature Publishing Group.
- 520 Tinbergen, N. (1953). *The herring gull's world: a study of the social behaviour of birds*. Frederick A. Praeger, Inc., Oxford, England.
- 520 Tyler, C. W., Baseler, H. A., Kontsevich, L. L., Likova, L. T., Wade, A. R., and Wandell, B. A. (2005). Predominantly extra-retinotopic cortical response to pattern symmetry. *Neuroimage*, 24(2):306–314.
- 520 van der Helm, P. A. and Leeuwenberg, E. L. J. (1996). Goodness of visual regularities: A nontransformational approach. *Psychological Review*, 103(3):429–456. Publisher: American Psychological Association.
- 520 von Fersen, L., Manos, C. S., Goldowsky, B., and Roitblat, H. (1992). Dolphin Detection and Conceptualization of Symmetry. In Thomas, J. A., Kastelein, R. A., and Supin, A. Y., editors, *Marine Mammal Sensory Systems*, pages 753–762. Springer US, Boston, MA.
- 520 Wade, D. (1993). *Crystal and Dragon: The Cosmic Dance of Symmetry and Chaos in Nature, Art and Consciousness*. Inner Traditions/Bear & Co.

- 655 Wagemans, J. (1998). Parallel visual processes in symmetry perception: Normality and pathology. *Dokumenta Ophthalmologica*, 95(3):359.
- 656 Webster, M. A. and MacLin, O. H. (1999). Figural aftereffects in the perception of faces. *Psychon Bull Rev*, 6(4):647–53.
- 657
- 658 Wagemans, J., Van Gool, L., and d'Ydewalle, G. (1991). Detection of symmetry in tachistoscopically presented dot patterns: effects of multiple axes and skewing. *Perception & Psychophysics*, 50(5):413–27.
- 659 Wright, D., Makin, A. D. J., and Bertamini, M. (2015). Right-lateralized alpha desynchronization during regularity discrimination: Hemispheric specialization or directed spatial attention? *Psychophysiology*, 52(5):638–647. _eprint: <https://onlinelibrary.wiley.com/doi/pdf/10.1111/psyp.12399>.
- 660
- 661
- 662 Watson, A. B. and Pelli, D. G. (1983). Quest: A bayesian adaptive psychometric method. *Perception & Psychophysics*, 33(2):113–120.
- 663
- 664
- 665
- 666
- 667
- 668
- 669
- 670
- 673